Separation Science and Technology
Publication details, including instructions for authors and subscription information:
http://www.informaworld.com/smpp/title~content=t713708471

Systematic Bench-Scale Assessment of Perchlorate (ClO_4^-) Rejection Mechanisms by Nanofiltration and Ultrafiltration Membranes

Yeomin Yoon[a]; Gary Amy[b]; Jaeweon Cho[c]; John Pellegrino[bd]
[a] Department of Mechanical Engineering, Northwestern University, Evanston, Illinois, USA [b] Department of Civil, Environmental, and Architectural Engineering, University of Colorado, Boulder, Colorado, USA [c] Department of Environmental Science and Engineering, Kwangju Institute of Science and Technology, Puk-gu, Kwangju, Republic of Korea [d] Physical and Chemical Properties Division, National Institute of Standards and Technology, Boulder, Colorado, USA

Online publication date: 08 July 2010

To cite this Article Yoon, Yeomin , Amy, Gary , Cho, Jaeweon and Pellegrino, John(2005) 'Systematic Bench-Scale Assessment of Perchlorate (ClO_4^-) Rejection Mechanisms by Nanofiltration and Ultrafiltration Membranes', Separation Science and Technology, 39: 9, 2105 — 2135
To link to this Article: DOI: 10.1081/SS-120039304
URL: http://dx.doi.org/10.1081/SS-120039304

SEPARATION SCIENCE AND TECHNOLOGY
Vol. 39, No. 9, pp. 2105–2135, 2004

Systematic Bench-Scale Assessment of Perchlorate (ClO_4^-) Rejection Mechanisms by Nanofiltration and Ultrafiltration Membranes[#]

Yeomin Yoon,[1] Gary Amy,[2] Jaeweon Cho,[3] and John Pellegrino[2,4,*]

[1]Department of Mechanical Engineering, Northwestern University, Evanston, Illinois, USA
[2]Department of Civil, Environmental, and Architectural Engineering, University of Colorado, Boulder, Colorado, USA
[3]Department of Environmental Science and Engineering, Kwangju Institute of Science and Technology, Puk-gu, Kwangju, Republic of Korea
[4]Physical and Chemical Properties Division, National Institute of Standards and Technology, Boulder, Colorado, USA

ABSTRACT

Measurements of the rejection of perchlorate anion (ClO_4^-) have been performed by using two thin-film composite nanofiltration (NF)

*Correspondence: John Pellegrino, Department of Civil, Environmental, and Architectural Engineering, University of Colorado, Campus Box 428, Boulder, CO 80309-0428, USA; E-mail: jjp@boulder.nist.gov.

DOI: 10.1081/SS-120039304 0149-6395 (Print); 1520-5754 (Online)
Published by Marcel Dekker, Inc. www.dekker.com

membranes and four ultrafiltration (UF) membranes. The latter four membranes are all from the same manufacturer and, ostensibly, from the same material family. These were chosen to systematically change the membranes steric properties, while keeping the same material chemistry, thus, the enthalpic interactions should stay constant. The perchlorate anion (at a concentration of 100 g/L of ClO_4^- by "spiking" with $KClO_4$) was presented to the membrane as a pure component, in binary mixtures with other salts, and at varying pH and ionic strength (conductivity). Also, a natural source water was "spiked" with perchlorate anion and used to document the effects of a complex mixture, including natural organic matter, on the observed rejection. All filtration measurements were performed at approximately the same permeate flow rate to minimize artifacts from mass transfer at the membrane interface. In general, the results indicate that, in a pure component system, target ions (in this case ClO_4^-) can be significantly excluded from like-charged membranes with pores large with respect to the size of the ion, but this rejection capability decreases in the presence of a sufficient amount of other ions that can screen the electrostatic force field.

Key Words: Nanofiltration; Perchlorate; Ultrafiltration; Water treatment.

INTRODUCTION

With the recent emergence of perchlorate (ClO_4^-) contamination as an important drinking-water quality issue, we performed a careful assessment of membrane technology for ClO_4^- removal. The scope of our measurements was to identify when and how higher productivity membranes—and, therefore, potentially, more economical ones—could provide useful levels of removal of ClO_4^- from the filtered water.

As a consequence of recent analytical developments, ClO_4^- contamination of drinking water sources has been discovered to be a significant problem. In the southwestern United States, ammonium perchlorate (NH_4ClO_4) has been widely used as an oxidizer in rocket fuel and is very stable when dissolved in water, in contrast to its high reactivity in the solid state. The California Department of Health Service (CDHS) has recently developed an analytical, ion chromatographic procedure for ClO_4^-, with a minimum detection limit of 2 μg/L. Based on a U.S. Environmental Protection Agency assessment of ClO_4^- toxicology, CDHS has defined a provisional action level—that is, the level of perchlorate at which, if it is exceeded, the CDHS advises water utilities to remove drinking water supplies from service—of 18 μg/L.[1] A ClO_4^- occurrence survey showed detectable ClO_4^- found in 69 of 232 well samples, with 24 exhibiting levels above

18 μg/L; samples derived from highly contaminated sites contained up to 8000–9000 μg/L.

Under the typical pH conditions of natural waters, perchlorate exists as an anion (ClO_4^-) associated with perchloric acid ($HClO_4$), a strong acid ($pK_a = -1.6$); ClO_4^- is the oxidation product of chlorate (ClO_3^-) and represents the highest oxidation state (+7) of the element chlorine, and ClO_4^- is an anion with a molecular mass of 100 and an ionic radius of $\sim 1.37 \times 10^{-10}$ m (estimated by using the Stokes–Einstein equation and its diffusion coefficient). The ionic radius of ClO_4^- is larger than that of OH^- (0.47×10^{-10} m) and Cl^- (1.21×10^{-10} m) and smaller than that of SO_4^{2-} (2.30×10^{-10} m).[2]

When a dilute solution containing ions is brought into contact with a membrane possessing a fixed charge, the passage of ions possessing the same charge as the membrane (co-ions) can be inhibited. This condition is termed Donnan exclusion.[3] The use of the extended Nernst–Planck model in conjunction with the Donnan equilibrium condition (with the effective membrane pore size and charge density) provides the possibility of predicting the separation of mixtures of electrolytes at the membrane/solution interface.[4] For example, Brandhuber[2] used the combined Donnan equilibrium/extended Nernst–Planck model to predict the rejections of arsenic species—As(III), a nonionic species, and As(V), an anion—by charged nanofiltration membranes at different feed water pHs and ionic compositions. The effective membrane charge depends on the bulk co-ion concentration and its valency.[4]

It has been known that if the pore dimensions are on the same order as those of a solute molecule, the solute's diffusion coefficient and concentration will differ from its value in the bulk solution. Solute transport typically is "hindered" or restricted at the membrane interface. In general, for solute transport through membranes, the diffusion coefficient is a harmonic average of the diffusion coefficients of ions, but the partition coefficient is a geometric average.[5] To study hindered transport is to seek to predict the applicable diffusion and partition coefficients from such fundamental information as the size, the shape, and the electrical charge of the solutes and pores.[6] Partition coefficients for solutes and pores of like-charge are affected by electrostatic interactions that depend on the solution's ionic strength—the partition coefficient increases with increasing ionic strength.[6] Malone and Anderson[7] determined the effects of electrostatic interactions on hindered diffusion by using latex particles in negatively charged porous membranes. In their study, effective diffusivity for the solute in membrane pores declined as ionic strength decreased. Since a species' transport is the product of its concentration and velocity in the membrane phase, the observed ionic transport (or rejection) in complex mixtures is not always straightforward to interpret.

This report presents membrane characterization measurements that reflect pore size, porosity, and surface charge, including effects from varying pH and overall solution ionic strength. These results then are qualitatively interpreted in the theoretical framework of the Donnan equilibrium and transport governed by the extended Nernst–Planck model to predict the trends in transport (rejection) of the trace ion ClO_4^- by the variety of membranes evaluated. These predictions then are compared with experimental measurements in a standard cross-flow membrane test apparatus.

The goal of this study was to verify whether existing theories and models were consistent with these bench-scale "figure-of-merit" transport measurements of rejection. The data and conclusions then can guide the development of transport parameters to be used in engineering correlations to predict scale-up results for pilot plant evaluations and can lead to better matching of membranes to process design objectives.

BACKGROUND

Nyström et al.[8] studied fouling and retention with four different NF membranes for different model substances. In their study, the membranes were first stabilized for ~4 hr with a pressure of 10 bar at 298 K, then the pure water flux of the membranes was measured. Stabilizing the membrane and then measuring its pure water permeability (PWP) is an important initial step before making other measurements, since it provides an indicator of overall porosity among membranes with similar apparent pore size.

It also is important to determine whether, and how much, the membrane pore sizes may vary in the presence of co- and counterions. Cho et al.[9] reported rejection tests with an uncharged species, polyethylene glycols (PEG), to determine the effects of the mono- and divalent ions, Cl^-, Na^+, and Ca^{2+}, on apparent membrane pore size. They found that a particular ultrafiltration (UF) membrane had a lower apparent molecular mass cutoff (MWCO) for PEGs in deionized water than in NaCl or $CaCl_2$ solutions. In that study, the UF membrane's nominal MWCO was 8000 but, in general, had an apparent MWCO above which the membrane rejects $\geq$90% of the molecules trying to pass through it—value greater than 8000 for the neutral, linear PEG macromolecules.

Electrostatic exclusion is known to be an important separation mechanism between charged solutes and membranes. Membrane surface charge can be estimated by measurements of the streaming potential and by calculating the associated zeta potential. The zeta potential is defined as the potential across the fluid shear plane near the membrane surface. Childress and Elimelech[10] studied the effects of pH and ions, Cl^-, SO_4^{2-}, Na^+, Ca^{2+}, and Mg^{2+}, on the

membrane surface charge of reverse osmosis (RO) and NF membranes. All of the membranes had a positive surface charge in the lower pH range, passed through an isoelectric point (zero charge) between pH 3 and pH 5, and then became negative in the mid- to high-pH range. In addition, the surface charge of a particular NF membrane (NF-70) became more negative in the presence of $CaCl_2$ and Na_2SO_4 salts.

It is intuitive that the measured surface charge depends on the functional groups associated with different membrane materials. An attenuated total reflection–Fourier transform infrared (ATR–FTIR) spectrum can sometimes be used to determine the membrane's functional groups. Cho et al.[11] previously presented the ATR–FTIR spectra of a UF (GM; see Table 1) and a NF (ESNA; see Table 1) membrane showing absorption peaks consistent with aromatic carbons and carboxylic acid groups. The latter groups provide a chemical basis for a negative surface charge.

A hydrodynamic operating parameter—the ratio of the initial pure-water flux (J_0) to the estimated back-diffusional mass transfer coefficient (k) through the boundary layer—can be used to facilitate comparison of results from different membranes in bench-scale, cross-flow flat-sheet tests.[12] If the permeate flux does not change throughout a measurement, then the concentration polarization (or ratio of solute concentration at the membrane surface to its value in the bulk solution, c_w/c_b) will be constant. Nonetheless, if membranes have different rejections for the solute, then their c_w/c_b will still

Table 1. Characteristics of the membranes.

Membrane ID	Material[a]	MWCO[b]	Ionizable groups[c]	PWP[d] ($L/d/m^2/kPa$)
ESNA	Polyamide TFC	200	Yes	1.05
MX07	Polyamide TFC	400	Yes	0.47
GH	Thin-film UF on polysulfone	2,500	Yes	0.74
GK	Thin-film UF on polysulfone	3,500	Yes	1.69
GM	Thin-film UF on polysulfone	8,000	Yes	2.81
GN	Thin-film UF on polysulfone	12,000	Yes	3.68

[a]Manufacturer's category.
[b]Based on PEG (manufacturer's data).
[c]Indicated by streaming potential determinations (our data).
[d]PWP is pure water permeability (our data).

differ somewhat. In this study, $J_0/k = 0.5$ has been used to perform all cross-flow flat-sheet tests. That is, the same test apparatus and approximately the same cross-flow velocity and permeate flow rate have been used to minimize artifacts due to differences of solute concentration at the membrane interface.

We used a model uncharged compound [an As(III) species] as a size surrogate to verify that incremental electrostatic exclusion occurs between anionic species and a negatively charged membrane. The As(III) exists as uncharged H_3AsO_3 at a pH < 9.13 ($pK_a = 9.13$) and its relative molecular mass $= 126$. Thus, it is comparable in size to ClO_4^- (relative molecular mass $= 100$), which is negatively charged at most pH conditions ($pK_a = -1.6$).

EXPERIMENTAL METHODS AND ANALYSIS

Membranes

The ClO_4^- rejection measurements were done on two NF and four UF membranes. The two NF membranes, ESNA and MX07, are thin-film composites made of aromatic polyamide (according to the manufacturer). These membranes have ionizable functional groups, such as unreacted carboxylic acids, and have different membrane pore sizes (assumed from the manufacturer's nominal MWCO). The four UF membranes, GH, GK, GM, and GN (all from the same manufacturer) are all made of the same proprietary surface material and, according to the manufacturer, only differ in their pore sizes (or nominal MWCO). These UF membranes were selected to systematically compare the results of steric exclusion for ClO_4^- rejection with the same material chemistry.

The surface charge of the ESNA, MX07, and G-series (using the GM as the representative sample) membranes were estimated by measuring streaming potential by using a commercial electrokinetic analyzer[a] (EKA) measurement apparatus. The PWP—which is related to pore size, pore density, and thickness—was determined over five different pressures for all the membranes used in our study. Table 1 lists the general membrane characteristics.

Source Waters

Two sources of water were used to perform bench-scale, cross-flow flat-sheet membrane tests. One source was Colorado River water (CRW) from

[a]Electrokinetic Apparatus-EKA, Brookhaven Instruments Corp., Holtsville, NY.

the Metropolitan Water District in California, and the other was ideal, model water solutions based on pure water with controlled salt compositions. The Colorado River, a major drinking water supply for southern California, southern Nevada, and Arizona, naturally contains 4–9 μg/L of ClO_4^-, with the Las Vegas Wash of Lake Mead identified as the major contamination source. Model water solutions were prepared with pure water from a commercial laboratory purification system[b] that uses deionization with two proprietary cation-exchange mixed beds and an anion-exchange bed followed by filtration through a 0.2-μm filter. The perchlorate anion (present at a concentration of 100 μg/L based on $KClO_4$) was fed to the membrane test apparatus either as a pure component or in binary mixtures with other salts (KCl, K_2SO_4, and $CaCl_2$) and at varying pH conditions (4, 6, 8, and 10) and solution conductivities (30, 60, and 115 mS/m). Potassium hydroxide (KOH) or hydrochloric acid (HCl) was added to the pure water to adjust solution pH. Unless otherwise indicated, the CRW was prefiltered with a 0.45-μm filter for all membrane tests.

Tables 2 and 3 list the characteristics of the feed waters used in this study. Several analyses were performed, including dissolved organic carbon (DOC), ultraviolet adsorption at 254 nm (UVA_{254})—a measure of natural organic matter (NOM) aromaticity—conductivity, total dissolved solids, and pH. The CRW represents relatively low NOM aromaticity based on its specific UVA_{254} ($SUVA = DOC/UVA_{254}$) value. The anions and cations in the CRW were measured to assess how the co- and counterions, Cl^-, SO_4^{2-}, K^+, and Ca^{2+}, would influence ClO_4^- rejection. As shown in Tables 2 and 3, the CRW has a relatively high conductivity from a variety of mono- and divalent ions; therefore, we would expect significant electrostatic screening to occur.

Continuous Cross-Flow Flat-Sheet Membrane Test Apparatus

Figure 1 shows a schematic of the experimental system used in the bench-scale, cross-flow flat-sheet tests. A commercial test cell[c] was used for these measurements. This cell permits testing of a single 9.5-cm × 14.6-cm^2 membrane swatch under tangential feed flow conditions with a channel height of 0.142 cm. The module has an active filtration area of ~139 cm^2 and without a spacer (which is how we used it), assuredly provides for a laminar flow condition. At our volumetric feed rate, the Reynolds number (*Re*) was ~35–78. (Note: due to the very different hydrodynamic environments, results in commercial scale equipment, especially with turbulence promoters, can vary from

[b]Milli-Q, Millpore Water Purification System, Bedford, MA.
[c]SEPA, Osmonics, Minnetonka, MN.

Table 2. Feed water characteristics.

Water	Conductivity (mS/m)	TDS (mg/L)	pH	DOC (mg/L)	UVA_{254} (1/cm)	SUVA (L/mg/m)	ClO_4 (μg/L)
CRW	115	541	8.1	2.25	0.036	1.6	3.8[b]/100[c]
Model water	30, 60, and 115[a]	N/A	4, 6, 8, and 10	N/A	N/A	N/A	100[c]

Note: N/A, not applicable; CRW, Colorado River water.
[a]Conductivity based on KCl, K_2SO_4, or $CaCl_2$ salt.
[b]Ambient ClO_4^- concentration in CRW.
[c]Total feed ClO_4^- concentration after spiking.

Table 3. Ions in CRW.

Anions	mg/L	Cations	mg/L	Other	mg/L
Cl^-	80.5	Na^+	216.7	SiO_2	31.8
SO^{-2}	248.8	Ca^{2+}	227.9		
NO_3^-	1.24	Mg^{2+}	118.9		
$HCO_3^{-\,a}$	79.3	K^+	4.8		
$CO_3^{-2\,a}$	0.94	Ba^{2+}	<0.1		

[a]Estimated with alkalinity measurements.

those measured in these bench-scale tests.) Table 4 presents the operating conditions for each membrane test. The experiments were performed at room temperature, 295 ± 1 K, and the initial transmembrane pressure was varied to obtain the $J_0/k = 0.5$. Our maximum available pump pressure forced us to operate the MX07 membrane tests at different feed and permeate flow rates to reach the target J_0/k.

To calculate a J_0/k, we needed to estimate the boundary layer back-diffusion mass transfer coefficient k. For this, we used the correlation for the mass transfer coefficient under laminar flow in a channel presented by Porter[13] and a ClO_4^- diffusion coefficient (D) of 1.79×10^{-5} cm^2/sec.[14] The correlation is

$$k = 1.177\left[\frac{U_b D^2}{hL}\right]^{1/3} \tag{1}$$

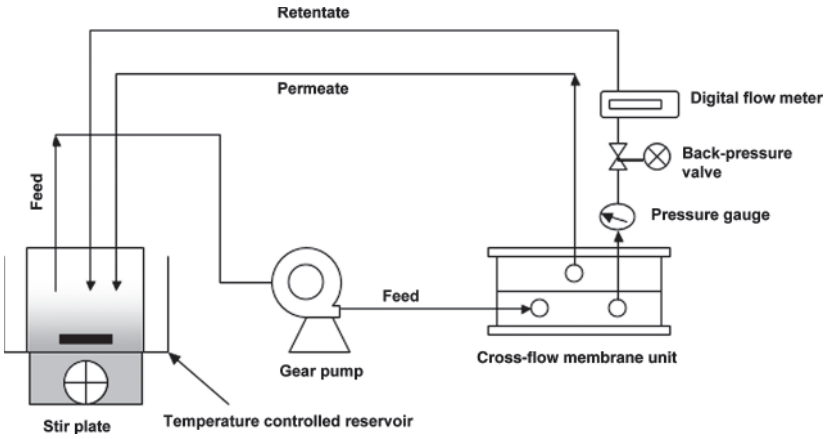

Figure 1. Schematic of cross-flow flat-sheet membrane filtration apparatus. *(View this art in color at www.dekker.com.)*

Table 4. Experimental operating conditions for cross-flow flat-sheet filtration.

Membrane	Transmembrane differential pressure (kPa) (psi)	Feed flow (mL/min)	Initial permeate flow (mL/min)	J_0 (cm/sec) $\times 10^4$	J_0/k	θ (%)[a]	U (cm/sec)[b]	Re
ESNA	366 (53)	225	5.8	7.0	0.5	2.6	5.6	78
MX07	614 (89)	100	4.4	5.3	0.5	4.4	2.5	35
GH	518 (75)	225	5.8	7.0	0.5	2.6	5.6	78
GK	228 (33)	225	5.8	7.0	0.5	2.6	5.6	78
GM	138 (20)	225	5.8	7.0	0.5	2.6	5.6	78
GN	104 (15)	225	5.8	7.0	0.5	2.6	5.6	78

[a]θ, percentage of volumetric recovery or permeate flow rate/feed flow rate.
[b]U, average crossflow velocity.

where U_b is the average cross-flow velocity of the feed fluid (cm/sec), h is the channel height (0.142 cm), and L is the channel length (14.6 cm).

Each new membrane tested was prefiltered with a non-recirculated pure-water feed volume of 8 L (at a feed flow rate of ~200 mL/min and a permeate flow rate of ~5 mL/min) to clean any humectant materials that may be coated onto/in the membrane surface/pores. Additionally, the new membrane then was soaked in pure water for at least 24 hr for further membrane stabilization. During this period, the pure water was replaced every 2–3 hr with a new volume of pure water. The new membrane was filtered again overnight with pure water, and the pure-water permeate flow was monitored for 3 hr just before each test until an approximately constant pure-water flux was obtained, only then was the test solution fed to the system. Unless otherwise indicated, all of the membranes used in the filtration tests, PEG rejection tests, and streaming potential measurements were prepared by using the prefiltraton methods described above.

The membrane PWP was evaluated over a pressure range of 69–550 kPa (10–80 psi) at ~295 K, the pure water fluxes increased with increasing pressure, and the slope provided the permeability—and is listed in Table 1.

The feed solution was drawn from a 4-L reservoir and was supplied to the flat-sheet test cell. The retentate and permeate streams were returned to the reservoir after passing through the test cell. The temperature of the feed solution was maintained within −1.0 K of the room temperature (~295 K) by immersing the reservoir in a temperature-controlled water bath. The feed waters were kept at room temperature for 24 hr prior to the filtration tests to assure thermal equilibration.[d] The retentate flow, permeate flow, and temperature were monitored over time, and the feed flow was calculated by summing the measured retentate and permeate flows. Duplicate analytical samples were taken every 15 min during ClO_4^- rejection tests. Rejection, R, was calculated based on the feed concentration, by using:

$$R = \frac{C_f - C_p}{C_f} \tag{2}$$

where C_f and C_p is perchlorate (or other solute) concentration in the feed and permeate, respectively.

[d]We don't expect any artifacts in our measurements of ion flux due to bacterial growth because we used either synthetic water solutions prepared from DOC-free water that was stored in bleach-sterilized, covered containers, or CRW that was prefiltered with a 0.45 μm filter before the tests.

Analytical Measurement of Perchlorate Concentration

The analytical method uses a commercial ion chromatography instrument[e] and associated columns to measure ClO_4^- concentration. All standards and solutions were made with 18 MΩ pure water (water free of dissolved organic carbon, anions, and cations). The ClO_4^- standards were made from potassium perchlorate, $KClO_4$. Sodium hydroxide for eluent was in a 50% (w/w) solution. The columns used were Dionex IonPac[f] AG11 guard ($4 \times 50\,mm^2$) column and a Dionex IonPac[f] AS11 analytical ($4 \times 250\,mm^2$) column. Five concentration standards of 1, 5, 20, 50, and 100 μg/L were used in the calibration. The instrument's internal software was used for data collection and running of the method.

A ClO_4^- calibration curve was constructed with the pure (>99%) standards, with the criterion for acceptance being a calibration curve with a linear coefficient of determination (r^2) of ≥0.95. The minimum reporting limit is 4 μg/L, while the method has a MDL of 1.4 μg/L. Uncertainty has been determined through replicate analyses with the resultant data used to calculate the mean and a standard deviation.

Co-ions, Cl^- and SO_4^{2-}, also were measured by using the same equipment but with an AS14-4 column. A 0.5 N $NaHCO_3$/0.5 N $NaCO_3$ eluent with a 50 mM H_2SO_4 regenerant was used with an injection volume of 250 μL. Counterions, K^+ and Ca^{2+}, were measured by using a inductively coupled plasma emission spectroscopy (ICP-ES) instrument.[g] A high purity standard solution with 1000 μg/μL potassium and calcium was used to make various standard solutions. The ICP-ES detects the spectra of ions excited by a high-temperature plasma at approximately 10,000 K.

MWCO Determination of the Membrane with PEG

PEG rejections for the ESNA, MX07, and GM membranes were performed with a range of PEGs[h] (relative molecular mass = 200–10,000) by

---

[e]DX300 Ion Chromatography System including a CDM-2 conductivity detector, a GPMII gradient pump, and an auto-sampler. Dionex Corp., Sunnyvale, CA.

[f]Manufacturer's identification is required to provide an accurate description of the instruments used for scientific purposes only. Identification is not intended to imply recommendation or endorsement by the National Institute of Standards and Technology, nor is it intended to imply that the equipment/materials used are the best available for the purpose.

[g]Liberty-Series II, Varian, Australia.

[h]Sigma, St. Louis, MO.

using a dead-end stirred-cell filtration unit. Total PEG concentrations varied between 5 and 6 mg/L as DOC for each of the four to five PEG rejection measurements. The PEG was introduced to the membrane as a single M_w component at pH 8 with conductivity <3.0 mS/m) and in mixtures with varying amounts of other salts (KCl, K_2SO_4, and $CaCl_2$) at pH 8. KOH and HCl were added to adjust the solution pH so that some KCl was always present. The overall solution conductivity (30, 60, and 115 mS/m) was used as the metric to change the salt concentration.

The experiments were performed at $\sim$295 K, and the pressure was varied to maintain the same permeate flow rate of $\sim$0.6 mL/min (and same stirrer speed) to minimize artifacts from mass transfer at the membrane interface. Each solution was filtered, and the permeate was discarded for 30 min to stabilize the transport. Then a permeate sample of 30 mL was collected for analysis by dissolved organic carbon measurement.[i] PEG rejection (by DOC analysis), based on initial feed concentration, was calculated by using Eq. (2) for each molecular mass component individually.

These measurements were performed, not strictly to estimate the MWCO of the membrane but to determine the effects of background electrolyte on rejection of a well-defined neutral species (the linear PEG macromolecule) due to changes (if any) of membrane pore geometry (size).

Streaming Potential Measurements

Streaming potential of the membrane surfaces (along the face of the membrane, not through the pores) were measured with an EKA. We followed the same procedures and used the same EKA to measure streaming potential as described by Wilbert et al.[15] The electrolyte solution was held in a jacketed reservoir kept at constant temperature by water circulated through a heating and cooling temperature-control bath. The external pH and conductivity sensors were placed in the electrolyte reservoir. Conductivity, temperature, pressure, and streaming potential were monitored with internal sensors. For the streaming potential measurements, the ESNA, MX07, and GM flat-sheet membrane samples were cut to fit the measurement cell and then wetted in a KCl, K_2SO_4, or $CaCl_2$ solution at the desired pH (4, 6, 8, and 10) and stored in a refrigerator for the presoaking time.

Zeta potential (ZP) was calculated from the measured streaming potential by using the method described by Fairbrother and Mastin,[16] which is based on the Helmholtz–Smoluchowski relationship, with the assumption that the

[i]TOC-5000, Shimadzu, Columbia, MD.

electrolyte solution, with conductivity k ($\Omega^{-1} \cdot m^{-1}$), carries most of the current. This approximation is acceptable for the membrane materials evaluated (and for ionic solutions $>10^{-3}$ M) and results in the following simplification:

$$\zeta = \frac{\Delta U \cdot \eta \cdot k}{\Delta P \cdot \varepsilon \varepsilon_0} \tag{3}$$

where ζ is the zp (mV), $\Delta U/\Delta P$ is the change in streaming potential with pressure ($mV \cdot Pa^{-1}$), η is the viscosity of the solution ($Pa \cdot sec$), ε_0 is the permittivity of free space ($sec \cdot m^{-1} \cdot \Omega^{-1}$), and ε is the dielectric constant of the solution.

RESULTS AND DISCUSSION

Membrane Characterization

PEG Rejection Measurements

The ESNA membrane has a greater PWP (see Table 1) than the MX07 membrane, even though the ESNA ostensibly has the smaller pore size (based on their nominal MWCOs). It is, therefore, reasonable to assume that the ESNA either has a greater pore density or a thinner pore layer (or some combination of the two) than the MX07. The PWPs of the UF membranes follow the order of their nominal MWCOs, GH < GK < GM < GN (see Table 1) as expected.

Figure 2 and Table 5 present the PEG rejection trends of the ESNA, MX07, and GM membranes at pH 8 with varying salt types and solution conductivities. All of the membranes show similar trends, that is, the PEG rejection (for a given M_w) increases with increasing conductivity. A possible explanation is compaction of the electrical double layer associated with the polymer matrix and, thus, a material relaxation that reduces the pore size. The results in Table 5 show that PEG rejection by the membranes varies with the specific salt and follows the order $KCl < K_2SO_4 \leq CaCl_2$. Apparently, the size and the valency of the ions affects the partitioning of the PEG into the membrane's pores. (We will see later that this ordering of the salt-type's effect is consistent with other measurements that depend on the extent of the electrostatic influence.) Figure 2 illustrates that the exclusion (rejection) of the lower molecular mass PEG fractions are the most influenced by the ionic nature of the solution. Also, for all three types of membranes, the variability of PEG rejection with the type and concentration of electrolyte is most apparent when the size of the PEG is small with respect to the nominal size of the membrane's "pores." If the nominal size of the membrane's pores decreases with increased

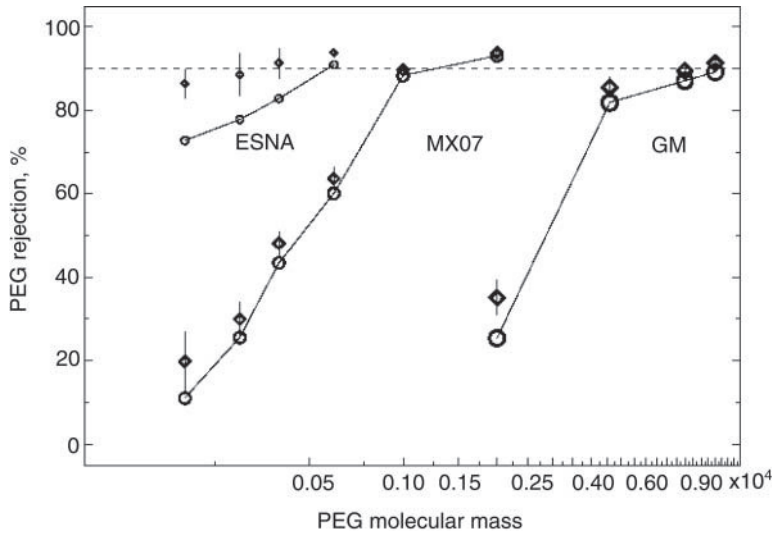

Figure 2. PEG rejection vs. PEG molecular mass for NF and UF membranes. The points (○) connected by lines are for solutions of PEG in DI H_2O. The points (◇) with error bars represent the average and 1 standard deviation of the PEG rejections for all the solutions and concentrations that contained salts as listed in Table 5.

conductivity, we can infer that the steric component of ClO_4^- rejection also may increase as the conductivity increases.

ZP Measurements

The ZP results were obtained at varying pH levels and conductivities and are listed in Table 6. These measurements establish the trends for the electrostatic contribution to ClO_4^- rejection from charge repulsion between it and the negatively charged membrane (under varying pH conditions and salts). The ZP for the ESNA and MX07 membranes are not significantly different from each other and are consistently more negative than the GM membrane (Figs. 3 and 4). The error bars for the GM membrane data are 1 standard deviation and reflect the relative uncertainty of the measurements. Figure 5 illustrates that the ZP also is affected by the different types of salt (see Table 6 for the complete data). At constant pH and solution conductivity, the absolute value of the membrane's ZP (it is always negative) follows the order $CaCl_2 < KCl < K_2SO_4$. However, the membranes exhibit less negative charge in higher conductivity solutions with all the salts. The pH exerts a major influence on the membrane surface charge, presumably, through ionizable

Table 5. PEG rejection results.

	% PEG rejection									
		KCl conductivity (mS/m)			K_2SO_4 conductivity (mS/m)			$CaCl_2$ conductivity (mS/m)		
PEG M_w	DI H_2O	30	60	115	30	60	115	30	60	115
ESNA										
200	73.0	80.4	82.3	84.5	86.6	88.4	89.6	88.8	88.9	89.2
300	78.0	85.4	85.3	86.5	92.8	93.2	94.1	89.3	90.8	91.8
400	82.9	89.8	90.3	91.4	94.7	95.0	95.3	90.3	91.3	92.7
600	91.0	92.4	93.2	94.9	95.9	95.4	95.7	91.6	93.5	95.1
MX07										
200	11.2	9.9	11.2	14.4	22.1	20.5	18.6	29.0	27.0	27.4
300	25.7	28.7	29.1	32.5	24.5	29.4	39.1	30.5	30.3	31.3
400	43.5	45.2	47.9	50.6	44.9	48.1	51.3	48.6	49.0	52.5
600	60.2	60.4	63.3	64.9	61.4	64.1	67.1	62.8	65.3	68.2
1,000	88.4	89.1	89.6	89.4	90.3	90.3	91.3	89.3	89.8	90.4
2,000	93.2	93.5	94.1	94.8	94.0	94.2	94.2	93.5	93.5	94.1
GM										
2,000	25.5	27.8	32.4	35.5	31.4	36.0	38.6	35.38	38.88	41.16
4,600	82.0	83.5	85.5	87.6	83.2	85.6	87.4	84.47	87.31	89.39
8,000	87.2	88.3	89.5	91.3	89.1	90.4	91.4	88.91	89.46	90.76
10,000	89.3	91.2	91.5	92.3	91.5	92.1	92.3	90.19	91.35	92.31

Table 6. Zeta potentials (ζ) of the membranes with respect to pH and conductivity.

pH	Conductivity (mS/m)	ζ (mV) ESNA	MX07	GM
			KCl	
4	30	−4.6	−5.6	−4.5
6	30	−13	−12.8	−8.85
8	30	−14.4	−13.9	−9.7
10	30	−15.5	−14.9	−10.65
8	30	−14.4	−13.9	−9.7
8	60	−11.5	−10.8	−7.2
8	115	−7.3	−6.9	−3.4
			K_2SO_4	
4	30	−8.4	−7.8	−5.85
6	30	−14.3	−14.8	−8.95
8	30	−17.2	−16.9	−10.2
10	30	−18.6	−18.1	−10.8
8	30	−17.2	−16.9	−10.2
8	60	−14	−14.2	−6.5
8	115	−10.5	−10.1	−5.9
			$CaCl_2$	
4	30	−4.3	−5.8	−3.2
6	30	−7.2	−7.4	−4.65
8	30	−8.8	−8.9	−5.65
10	30	−9.7	−9.4	−6.7
8	30	−8.8	−8.9	−5.65
8	60	−7.1	−7.4	−4.95
8	115	−5.3	−5.8	−3.35

species, and many previous studies reported that both pH and ion composition affect the surface charge of RO and NF membranes.[10,17] All three tested membranes acquired more negative charge when pH increased at constant conductivity (30 mS/m), regardless of the salt.

These results are all consistent with trends expected from the simple theories of electrokinetic phenomena, that is, both higher salt concentration (conductivity) and higher ionic valency decreases the Debye length, thus, lowering the ZP. The manner in which other factors, such as the relative dielectric strength of the different ion solutions, co-ion binding, and counterion mobility, that would affect the ZP are also consistent with these measurements. For example, the ZP of membranes is decreased by $CaCl_2$ due to it being a divalent co-ion,

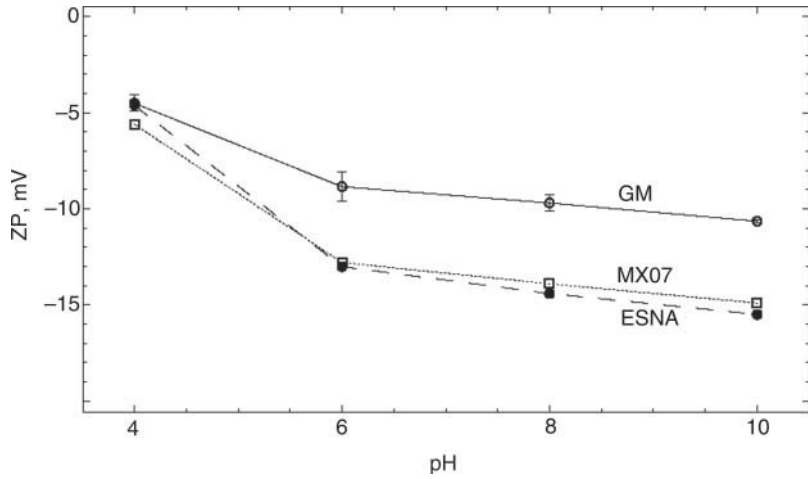

Figure 3. Effect of pH on zeta potential for the NF and UF membranes with KCl at a conductivity of 30 mS/m.

with stronger ion complexation (binding) with surface groups. We also interpret that adsorption of Cl^- co-ion (in hydrophobic regions) also is reduced with increasing conductivity (ionic strength) due to the decrease of the electrical double layer (due to fixed ionizable groups). We also can apply this interpretation

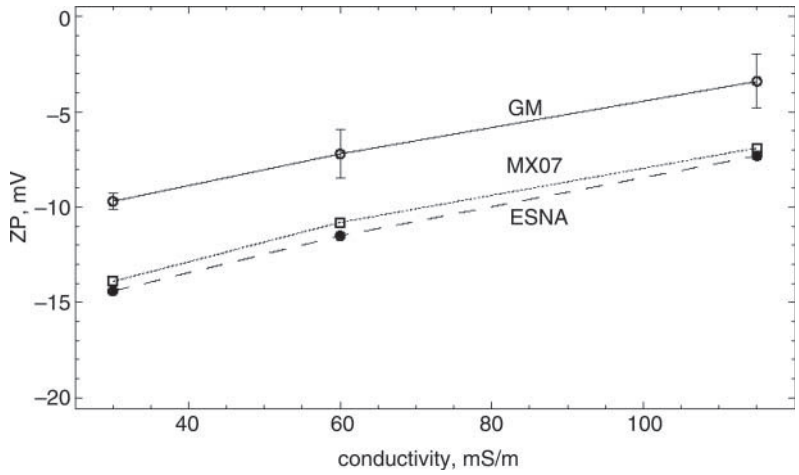

Figure 4. Effect of conductivity on zeta potential for the NF and UF membranes with KCl at a pH = 8.

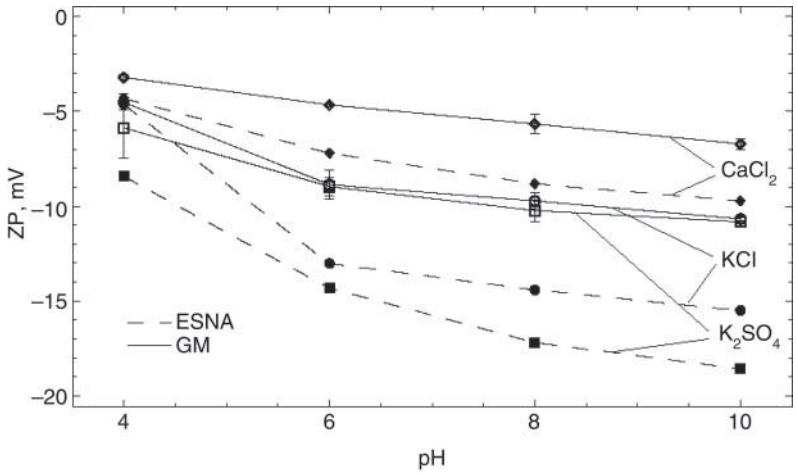

Figure 5. Influence of electrolyte salt type on the zeta potential variation with pH. Two membranes are presented: GM (open symbols and solid line) and ESNA (closed symbols and dashed lines).

to a divalent co-ion, like SO_4^{2-}; SO_4^{2-} bonding/adsorption can significantly decrease even with increasing K_2SO_4 concentration due to a decrease in the electrical double layer, since the SO_4^{2-} bonding/adsorption occurs mostly in the inner plane, which is affected by the size of the electrical double layer.

Overall, independent of the type of mono- and divalent co- and counterions, the ZP of the membranes become less negative (almost linearly) with increasing solution conductivity at pH = 8. Our results and interpretations are consistent with the general observations of previous studies that explain the effects of pH and co- and counterions on the ZP of RO and NF membranes with the following phenomena:

1. In aqueous solutions, since anions are less hydrated than cations, they can more closely approach the membrane surface.[10]
2. Preferential adsorption of anions has been used to explain surface charge behavior of several non-ionic surfaces (that is, surfaces without ionizable functional groups).[10]
3. Since thin-film composite membranes are made by the interfacial polymerization reaction of a monomeric polyamine with a polyfunctional acyl halide, anionic surface functional groups are expected.[18,19]
4. In surface complex formation, the ion may form an inner-sphere complex (coordinating bond) and an outer-sphere ion pair, or may be in the diffuse layer of the electrical double layer.[20]

5. If electrostatic attraction is the only association mechanism, the Ca^{2+} would form an outer-sphere complex. However, if co-ion bonding (or some combination of co-ion and ionic bonding) occurs, inner-sphere complexes are formed.[9]

ATR–FTIR Measurements for Surface Functional Groups

The ATR–FTIR[j] spectra of unused ESNA, MX07, and GM membranes are shown in Fig. 6. All the membranes show almost the same spectral pattern with slightly different intensities even though the ESNA and MX07 membranes are composed of an aromatic polyamide (TFC) and the GM membrane is composed of polyethersulfone (PES) with an ultrathin (~50–100 Å) proprietary top layer according to the manufacturer.

In general, a TFC membrane is made of three parts, top layer, microporous support, and support. The microporous support is often polysulfone or PES. The ATR–FTIR integrates the absorption from a layer on the order of the penetration depth of the evanescent wave (~1000–10,000 Å), thus, the top layer is too thin to obtain differentiated peaks because the evanescent wave passes through it and primarily loses energy in the microporous support. As shown in Fig. 6, the indicative characteristic FTIR peaks for polysulfone are seen at 1592 and 1110 cm^{-1} (aromatic double bonded carbons); at 1016 cm^{-1} (ether); at 1492 cm^{-1} (methyl); and at 1151 and 694 cm^{-1} (sulfone).[21] Thus, the only thing we can safely assume is that all the membranes are based on polysulfone-type microporous support layers.

Only the ZP results can support an assumption that the ESNA, MX07, and GM (G-series) membranes have ionizable functional groups, since the ATR–FTIR spectra do not directly show these groups.

Expectations with Respect to Perchlorate Transport

Several qualitative predictions for the perchlorate ion transport through these membranes can be made from the characterizations with PEG rejection and streaming potential measurements:

1. ClO_4^- rejection may increase with increasing conductivity only due to decreasing membrane pore size, which contributes to size exclusion,

[j]Magna-IR750 Spectrometer Series II, Nicolet Analytical Inst. Corp., Madison, WI.

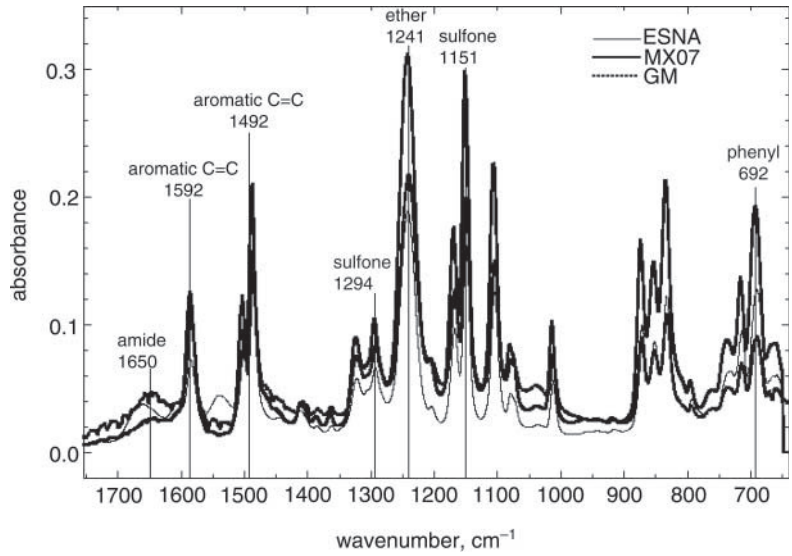

Figure 6. Comparison of FTIR spectra of clean NF and UF membranes.

particularly for the relatively smaller pore size membranes (ESNA and MX07).

2. ClO_4^- rejection increases (due to more electrostatic repulsion) with increasing pH due to the increasingly negative membrane surface charge (based on ZP).
3. ClO_4^- rejection decreases (due to less electrostatic repulsion) with increasing solution conductivity due to a less negative membrane surface charge (based on ZP).

ClO_4^- Rejection and Flux-Decline with Pure Water and CRW

Measurements of ClO_4^- rejection by the ESNA, MX07, and GM membranes were made for 22 hr. The pure water (at pH 8.1 and conductivity $<3.0\,mS/m$) was spiked with $100\,\mu g/L$ ClO_4^-, and the CRW with $96\,\mu g/L$ (since it already contained $\sim 4\,\mu g/L$). Flux-decline trends were also monitored at the same time. In Tables 2 and 3, the feed water composition of CRW (including the ions) are presented. Table 4 presents the experimental operating conditions for the cross-flow, flat-sheet filtration for the various membranes. All of the membranes showed relatively high (75–90%) ClO_4^- rejection in pure water. Also, the ESNA membrane

consistently had 80% ClO_4^- rejection over time with CRW, which was higher than that observed for either the MX07 (~25%) or the GM (<5%) membranes (see Fig. 7). Also, in our work, ClO_4^- rejection did not appear to be affected by the flux-decline during these short-term bench-scale filtration tests; however, detailed monitoring of this effect was not a focus of the current study.

The CRW was selected as a model, natural feed water, since it already contained small amounts of ClO_4^-, has been widely used as a drinking water source, and has relatively high levels of other typical anions and cations. From the results, both steric (size) and electrostatic interactions significantly contributed to ClO_4^- rejection with the relatively small-pore-size and negatively charged ESNA membrane. Only electrostatic repulsion can be a dominant mechanism for ClO_4^- rejection from the model waters for the relatively large-pore size MX07 and GM membranes. The ClO_4^- rejection with these membranes was significantly reduced when filtering CRW compared to the ideal model water with lower ion content. The ions in the CRW cause the ZP of those membranes to decrease; thus, electrostatic repulsion of the ClO_4^- decreases. This is consistent with our expectations from the membrane characterization measurements.

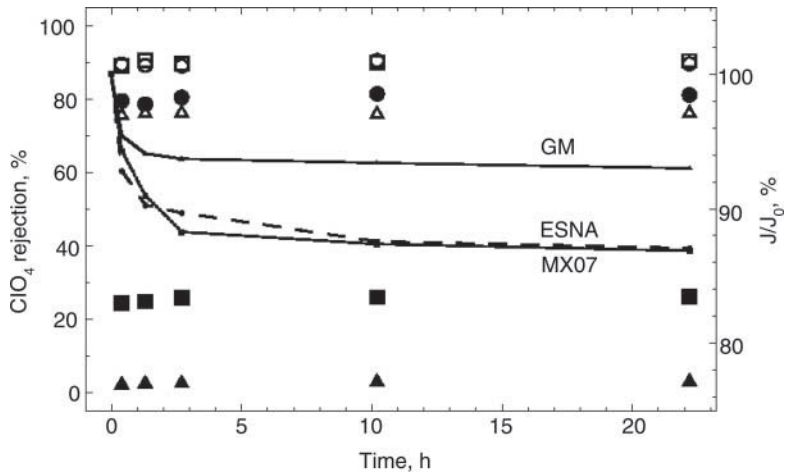

Figure 7. Comparison of perchlorate rejection (open symbols are DI water solutions and filled symbols are with spiked-CRW solutions) and flux-decline trends (—) with CRW for the NF (ESNA are circles and MX07 are squares) and UF (GM are triangles) membranes.

Detailed Results of ClO_4^- Rejection at Varying pH and Conductivity in Pure Water

The effects on ClO_4^- rejection by the ESNA, MX07, GH, GK, GM, and GN membranes with changes in solution pH and conductivity were determined with the ideal model water having three different salts (KCl, K_2SO_4, and $CaCl_2$) as the primary background electrolyte. These results are presented in Table 7. Figure 8 presents the ClO_4^- rejection results with KCl as the background electrolyte (and includes the 1 standard deviation uncertainty limits for the ESNA and MX07 membrane measurements). Regardless of the salt type, ClO_4^- rejection increases with increasing pH, (at a constant

Table 7. Rejection (%) of ClO_4^- in DI H_2O (and the indicated background electrolyte) with respect to pH and conductivity.

pH	Conductivity (mS/m)	ESNA	MX07	GH	GK	GM	GN
				KCl			
4	30	63.6	39.3	40.7	31.6	24.2	22.0
6	30	76.4	45.6	48.1	32.7	24.9	22.5
8	30	84.5	57.0	52.1	34.4	26.3	26.6
10	30	89.4	65.6	62.4	49.5	32.6	37.2
8	30	84.5	57.0	52.1	34.4	26.3	26.6
8	60	83.4	43.9	49.5	28.4	20.6	18.8
8	115	81.3	26.7	37.0	23.5	12.4	13.6
				K_2SO_4			
4	30	40.6	23.2	38.9	32.0	10.8	4.6
6	30	69.7	32.9	58.8	35.9	13.4	10.9
8	30	78.9	42.5	60.8	36.5	13.7	12.2
10	30	86.0	60.5	65.9	48.2	23.8	19.9
8	30	78.9	42.5	58.8	36.5	13.7	12.2
8	60	83.3	37.2	51.2	17.1	8.1	3.7
8	115	75.4	13.1	28.2	0.8	0.9	1.5
				$CaCl_2$			
4	30	53.5	12.8	14.2	2.1	1.9	0.7
6	30	59.3	17.1	17.4	3.6	3.3	1.8
8	30	62.9	18.2	22.2	7.4	4.0	2.2
10	30	67.3	21.1	23.6	6.3	4.9	2.5
8	30	62.3	15.1	22.2	7.4	4.0	2.2
8	60	67.9	14.2	12.1	3.5	3.1	1.2
8	115	64.2	13.4	9.0	1.1	2.3	0.7

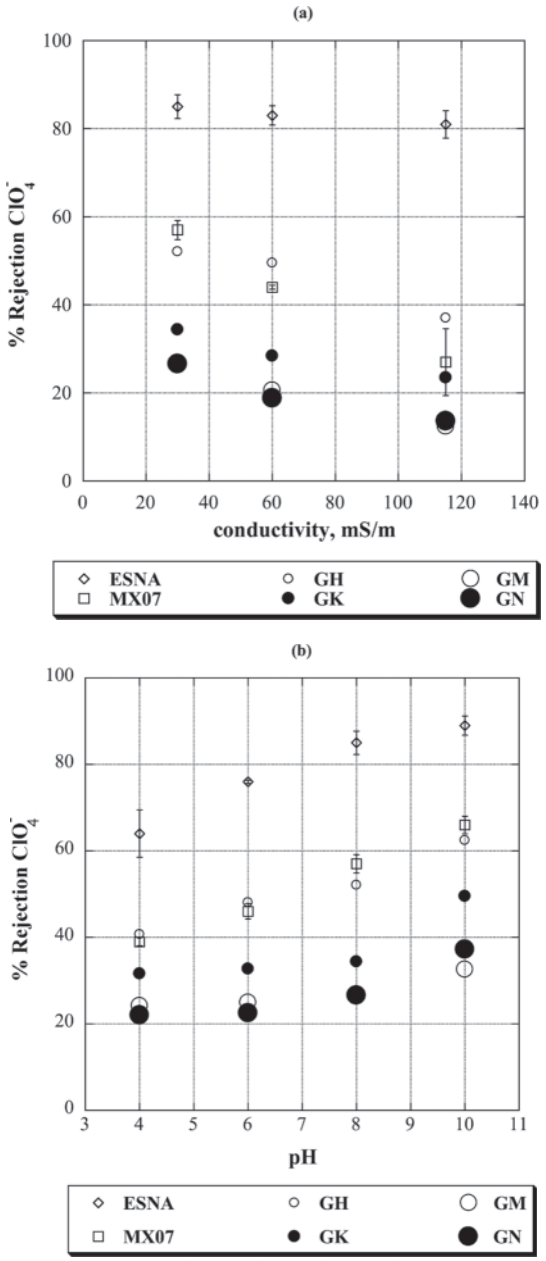

Figure 8. Effect of pH on perchlorate rejection for the NF and UF membranes with variable salts, KCl, K_2SO_4, and $CaCl_2$.

conductivity = 30 mS/m) for all the membranes. This is possibly attributable to OH^- adsorption occurring in the inner plane at the membrane surface[22] or a greater degree of disassociation of fixed ionizable moieties in the membrane. The ClO_4^- rejection follows the order $CaCl_2 < K_2SO_4 < KCl$ at constant pH and conductivity conditions for all the membranes tested.

In terms of electrostatic interactions, the Ca^{2+} binding causes the membrane's surface charge to decrease significantly in absolute value, thus ClO_4^- rejection is much lower in solutions having $CaCl_2$ than in those with KCl and K_2SO_4. The ClO_4^- rejection is greater with the KCl solution than with the K_2SO_4 solution, even though the apparent ZP is greater with the K_2SO_4 solution than with the KCl solution. These results are opposite to the prediction based simply on electrostatic interactions and the measured ZP results.

We rationalize these results by realizing that K_2SO_4 will be excluded by all the membranes to a greater extent than KCl (divalent vs. monovalent anion), thus, with concentration polarization, the K_2SO_4 concentration at the membrane interface increases more than that of the KCl during filtrations. (These anion rejection results for the GH, GK, GM, and GN membranes are presented in Table 8.) The ZP measurements clearly illustrated the effect of salt concentration on the dielectric screening, thus, it is reasonable to interpret that with greater interfacial concentration in the case of K_2SO_4 vs. KCl as the background electrolyte, the electrical double layer is more reduced with K_2SO_4. Thus, the effective electrostatic field exerted on ClO_4^- at the interface of the membrane during filtration is more negative when KCl is the background electrolyte vs. K_2SO_4.

The ClO_4^- rejection follows the order GN < GM < GK < GH < MX07 < ESNA at all pH conditions. These results are consistent with the influence of pore size on both steric and electrostatic effects based on their nominal MWCOs, ESNA < MX07 < GH < GK < GM < GN.

The ClO_4^- rejection decreases with increasing solution conductivity [for example see Fig. 8(a)] for all the membranes (the ESNA is the least affected.) We infer that these results are due to a reduction in electrostatic repulsion, and the corresponding increase in both the hindered diffusion and partitioning (between the ClO_4^- and the membrane) with increasing conductivity.

Effects of Co- and Counterion Rejection on Perchlorate Transport

The concentration of each co- and counterion species, K^+, Ca^{2+}, Cl^-, and SO_4^{2-}, as well as ClO_4^- in the feed and permeate during filtration was

Table 8. Rejection (%) of the anion (from the background electrolyte) with respect to pH and conductivity.

pH	Conductivity (mS/m)	GH	GK	GM	GN
			Cl^- (KCl)		
4	30	43.5	28.7	15.3	6.7
6	30	43.9	32.1	16.3	13.7
8	30	54.7	39.6	16.9	14.2
10	30	81.4	43.9	20.5	34.7
8	30	54.7	39.6	16.9	14.2
8	60	50.3	37.3	15.7	11.3
8	115	49.3	27.5	5.8	2.1
			SO_4^{2-} (K_2SO_4)		
4	30	77.8	87.6	87.8	73.8
6	30	79.3	87.9	88.3	78.0
8	30	81.4	88.5	88.2	80.3
10	30	83.4	88.6	90.1	85.1
8	30	81.4	88.5	88.2	80.3
8	60	81.3	80.8	80.6	58.1
8	115	76.8	78.7	66.3	33.4
			Cl^- ($CaCl_2$)		
4	30	7.5	1.8	8.1	1.3
6	30	14.6	2.3	8.8	2.2
8	30	26.2	2.5	8.5	2.1
10	30	28.8	3.6	9.8	3.9
8	30	26.2	2.5	8.5	2.1
8	60	20.9	2.2	4.2	1.1
8	115	15.5	1.7	2.7	0.5

measured to determine how the target solute's composition at the interface of the membranes may change and to provide a more complete ion transport data set for future theoretical modeling. These measurements were done for filtration with the GH, GK, GM, and GN membranes (see Tables 8 and 9). The measurements were performed at varying pH and solution conductivity. (The experimental conditions, pressure, feed flow rate, permeate flow rate, J_0/k, recovery, and cross-flow velocity, were as previously described in Table 4.)

When dilute solutions containing Cl^- or SO_4^{2-} anions are brought in contact with a membrane possessing a fixed negative charge, the Donnan

Table 9. Rejection (%) of the cation (from the background electrolyte) with respect to pH and conductivity.

pH	Conductivity (mS/m)	GH	GK	GM	GN
			K^+ (KCl)		
4	30	39.3	31.9	19.4	21.6
6	30	44.1	33.5	21.0	21.2
8	30	48.9	35.9	24.1	18.4
10	30	53.7	35.1	24.3	29.1
8	30	49.6	35.9	24.1	18.4
8	60	51.9	35.1	17.3	18.5
8	115	45.8	27.5	8.6	2.6
			K^+ (K_2SO_4)		
4	30	63.6	75.0	81.6	58.8
6	30	76.6	74.9	83.1	68.7
8	30	76.9	76.6	83.9	70.6
10	30	72.7	77.2	83.3	74.6
8	30	76.6	76.6	83.9	70.6
8	60	76.9	77.8	73.0	58.3
8	115	75.6	75.5	63.0	28.9
			Ca^{2+} ($CaCl_2$)		
4	30	24.9	8.7	4.1	3.2
6	30	21.0	8.3	3.9	2.0
8	30	24.9	8.5	4.3	2.4
10	30	28.3	9.6	4.7	1.6
8	30	15.5	8.5	4.3	2.4
8	60	27.2	5.5	1.1	2.9
8	115	20.5	2.4	0.9	1.1

exclusion provides that rejection of chloride and sulfate may be greater than if the membrane were completely uncharged. Also, we mentioned earlier how Ca^{2+} binding screens the co-ion adsorption. When the charge screening by Ca^{2+} occurs for the negatively charged membranes, anion rejection is significantly reduced.

The background electrolyte's cation and anion rejections vary from 2% to 90%, depending on the pH and conductivity and follow the same trends as the ClO_4^-. The background ion concentration at the membrane interface influences the further Donnan exclusion. As discussed previously, the ClO_4^- rejection is reduced because of the effect on the electric double layer from increased concentration of the other ions, K^+, Cl^-, and SO_4^{2-} when some

concentration accumulation occurs. For example, SO_4^{2-} is rejected more than the monovalent co-ion Cl^-, and K^+ is rejected to a greater degree in the presence of SO_4^{2-} than in the presence of Cl^- (due to the requirement of electroneutrality). These ion rejection results are consistent with the trends anticipated from the ZP results shown in Table 6 and Figs. 3–5. Thus, the influence of conductivity (or concentration) on the ZP provides a self-consistent framework for our observations of the magnitude of electrostatic repulsion that different ionic solutes would experience at the membrane interface.

The Effect of ZP on Neutral As(III) Rejection

We used a model uncharged species, As(III), to further confirm that electrostatic repulsion between anionic species and a negatively charged membrane is contributing to the observed transport results, and that steric/size exclusion mechanism is more dominant for the ESNA than for the MX07 membrane. The measurements were performed by using only KCl as the background electrolyte but with varying pH and conductivity—as when ClO_4^- was the trace component (see Fig. 8). The As(III) rejection only slightly varies (see Fig. 9) over the range of conductivities when the pH < 10, since the As(III) exists primarily as an uncharged species below pH 9.13. However, As(III) rejection significantly increases at pH 10 when it becomes anionic As(V). The ClO_4^- rejection is significantly greater at the same pH and conductivity conditions than As(III). Steric/size exclusion is the determining mechanism for the uncharged As(III) species until it becomes anionic at pH > 9.13—where the electrostatic exclusion mechanism begins to play a role.

CONCLUSIONS

The ClO_4^- rejection by negatively charged NF and UF membranes is significantly greater than expected based solely on steric/size exclusion due to electrostatic (Donnan) exclusion. This mechanism of exclusion, though, significantly decreases in a consistent fashion with the presence of background electrolytes, that reduce the negative membrane surface charge. Even though background electrolytes affected the absolute size exclusion of the membranes—as evidenced by measurements done with neutral PEG molecules—this was too small of an effect to be contributory in the case of the ClO_4^- transport. For the particular charged NF and UF membranes we studied, the perchlorate anion is primarily rejected by

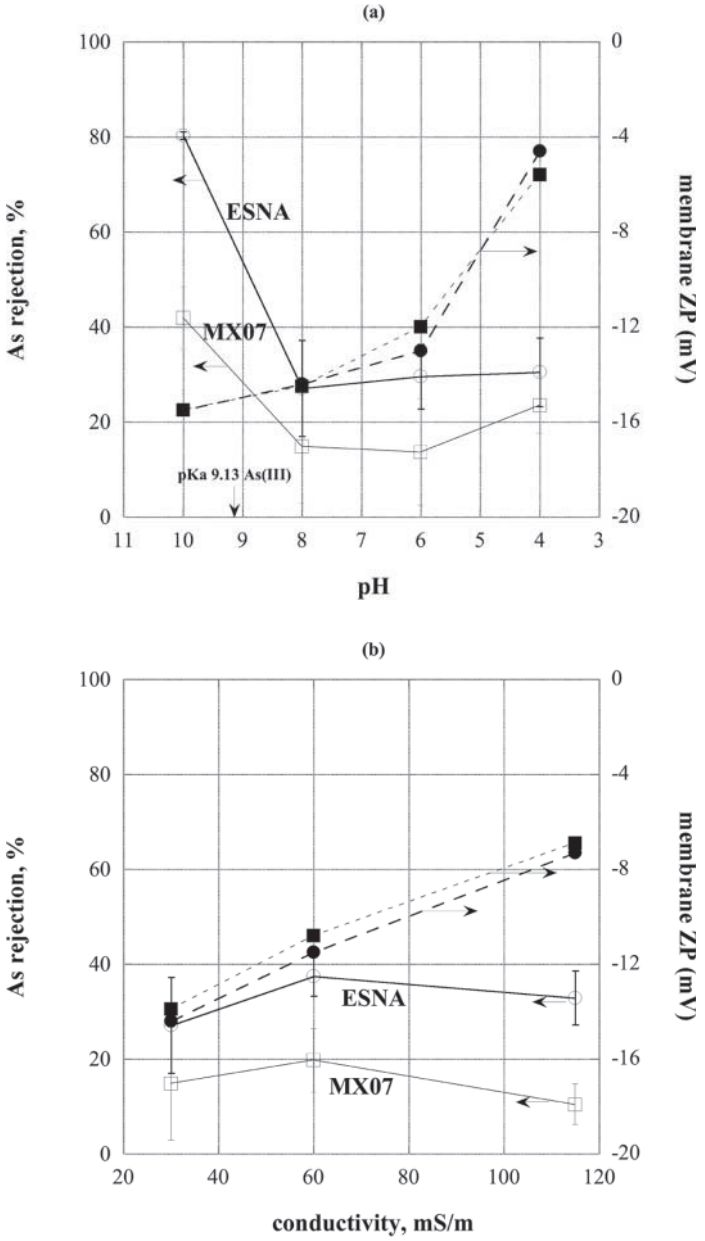

Figure 9. Effect of salts, KCl, K_2SO_4, and $CaCl_2$ on perchlorate rejection for the NF and UF membranes.

electrostatic exclusion, and the trends follow theoretical understanding. Data on mixed ion rejection (transport) has been presented to facilitate further theoretical modeling efforts.

ACKNOWLEDGMENTS

The authors wish to acknowledge the American Water Works Association Research Foundation (Ms. Traci Case, project manager) for support of this project and Namguk Her for doing the FTIR measurements.

REFERENCES

1. EPA *Perchlorate Environmental Contamination: Toxicological Review and Risk Characterization Based on Emerging Information*; EPA, Report; NCEA-1-0535, 2002.
2. Brandhuber, P. The Application of Pressure Driven Membrane Filtration as a Means of Arsenic Removal for Public Drinking Water Supply Systems. Department of Civil, Environmental, and Architectural Engineering, University of Colorado at Boulder; 1999; Ph.D. Dissertation.
3. Strathmann, H. *Membrane Handbook*; Ho, W.S., Sirkar, K.K., Eds.; Van Nostrand Reinhold; 1992.
4. Bowen, W.R.; Mukhtar, H. Characterisation and prediction of separation performance of nanofiltration membranes. J. Memb. Sci. **1996**, *112*, 263–274.
5. Cussler, E.L. *Diffusion Mass Transfer in Fluid Systems*, 2nd Ed.; Cambridge University Press; 1997.
6. Deen, W.M. Hindered transport of large molecules in liquid-filled pores. J. AIChE. **1987**, *33* (9), 1409–1425.
7. Malone, D.M.; Anderson, J.L. Diffusional boundary-layer resistance for membranes with low porosity. J. AIChE **1977**, *23*, 177–184.
8. Nystrom, M.; Kaipia, L.; Luque, S. Fouling and retention of nanofiltration membranes. J. Memb. Sci. **1995**, *98*, 249–262.
9. Cho, J.; Amy, G.; Pellegrino, J. Membrane filtration of natural organic matter: factors and mechanisms affecting rejection and flux-decline with charged ultrafiltration (UF) membrane. J. Memb. Sci. **2000**, *164*, 89–110.
10. Childress, A.; Elimelech, M. Effect of solution chemistry on the surface charge of polymeric reverse osmosis and nanofiltration membranes. J. Memb. Sci. **1996**, *119*, 253–268.

11. Cho, J.; Amy, G.; Pellegrino, J.; Yoon, Y. Characterization of clean and natural organic matter (NOM) fouled NF and UF membranes, and foulants characterization. Desalination **1998**, *118*, 101–108.
12. Cho, J.; Amy, G.; Pellegrino, J. Membrane filtration of natural organic matter: initial comparison of rejection and flux decline characteristics with ultrafiltration and nanofiltration membranes. Wat. Res. **1999**, *33* (11), 2517–2526.
13. Lide, D.R. *CRC Handbook of Chemistry and Physics*, 76th Ed.; Lide, D.R., Ed.; CRC Press; 1995–1996; 5–91.
14. Porter, M.C. Concentration polarization with membrane ultrafiltration. Ind. Eng. Chem. Prod. Res. Dev. **1972**, *11* (3), 234–248.
15. Wilbert, M.C.; Delagah, S.; Pellegrino, J. Variance of streaming potential measurements. J. Memb. Sci. **1999**, *161*, 247–261.
16. Fairbrother, F.; Mastin, H.J. Studies in electro-endosmosis. Chem. Soc. **1924**, *125*, 2319–2323.
17. Hong, S.; Elimelech, M. Chemical and physical aspects of natural organic matter (NOM) fouling of nanofiltration membranes. J. Memb. Sci. **1997**, *132*, 159–181.
18. Petersen, R.J.; Cadotte, J.E. Thin film composite reverse osmosis membranes. In *Handbook of Industrial Membrane Technology*; Porter, M.C., Ed.; Noyes Publications: Park Ridge, NJ, 1990; 307–348.
19. Elimelech, M.; Chen, W.H.; Waypa, J.J. Measuring the zeta (electrokinetic) potential of reverse osmosis membranes by a streaming potential analyzer. Desalination. **1994**, *95*, 269–285.
20. Stumm, W. *Chemistry of the Solid–Water Interface*; Wiley: New York, 1992.
21. Bellamy, L.J. *The Infra-Red Spectra of Complex Molecules*; Chapman and Hall: London, 1975.
22. Elimelech, M.; O'Melia, C.R. Effect of electrolyte type on the electrophoretic mobility of polystyrene latex colloids. Colloids Surf. **1990**, *44*, 165–178.